

The Giant Magellan Telescope Adaptive Optics Program

Antonin H. Bouchez^{*a}, D. Scott Acton^b, Carmelo Arcidiacono^c, Guido Agapito^c, Francis Bennet^d, Valdemaro Biliotti^c, Marco Bonaglia^c, Runa Briguglio^c, Guido Brusa-Zappellini^c, Lorenzo Busoni^c, Luca Carbonaro^c, Johanan L. Codona^f, Rodolphe Conan^d, Tom Connors^f, Celine d'Orgeville^d, Oli Durney^f, Brady Espeland^d, Simone Esposito^c, Luca Fini^c, Rusty Gardhouse^d, Thomas M. Gauron^g, Michael Hart^f, Phillip M. Hinz^f, Srikrishna Kanneganti^g, Edward J. Kibblewhite^h, Russell Knox^f, Brian A. McLeod^g, Tom McMahon^f, Manny Montoya^f, Timothy J. Norton^g, Mark Ordway^g, Simon Parcell^d, Piotr Piatrou^d, Enrico Pinna^c, Ian Price^d, Fernando Quiros-Pacheco^c, Alfio Puglisi^c, Armando Riccardi^c, John Roll^g, Gelys Tranco^a, Kristina Uhlendorf^d, Vidhya Vaitheeswaran^f, Marcos A. van Damⁱ, Dave Weaver^g, Marco Xompero^c

^aGMTO Corp., 251 S. Lake Ave., Pasadena, CA, USA 91101; ^bBall Aerospace & Technologies Corp, 1600 Commerce St., Boulder, CO, USA 80306; ^cArcetri Astrophysical Observatory, Largo Enrico Fermi 5, Firenze, Italia 50125;

^dResearch School of Astronomy and Astrophysics, The Australian National University, Cotter Road, Weston, ACT, Australia 2611; ^eLBT Observatory, Univ. of Arizona, 933 N Cherry Ave., Tucson, AZ, USA 85721; ^fSteward Observatory, Univ. of Arizona, 933 N. Cherry Ave., Tucson, AZ, USA 85721; ^gSmithsonian Astrophysical Observatory, 60 Garden St., Cambridge, MA, USA 02139; ^hDept. of Astronomy and Astrophysics, Univ. of Chicago, 5640 S. Ellis Ave., Chicago, IL, USA 60637; ⁱFlat Wavefronts, P.O. Box 1060, Christchurch, New Zealand 8140;

ABSTRACT

The Giant Magellan Telescope adaptive optics system will be an integral part of the telescope, providing laser guide star generation, wavefront sensing, and wavefront correction to most of the currently envisioned instruments. The system will provide three observing modes: Natural Guidestar AO (NGSAO), Laser Tomography AO (LTAO), and Ground Layer AO (GLAO).

All observing modes will use the telescope's segmented adaptive secondary mirror to deliver a corrected beam directly to the instruments. High-order wavefront sensing for the NGSAO and LTAO modes is provided by a set of wavefront sensors replicated for each instrument and fed by visible light reflected off the cryostat window. An infrared natural guidestar wavefront sensor with open-loop AO correction is also required to sense tip-tilt, focus, segment piston, and dynamic calibration errors in the LTAO mode. GLAO mode wavefront sensing is provided by laser guidestars over a ~ 5 arcminute field of view, and natural guidestars over wider fields. A laser guidestar facility will project 120 W of 589 nm laser light in 6 beacons from the periphery of the primary mirror. An off-axis phasing camera and primary and secondary mirror metrology systems will ensure that the telescope optics remain phased.

We describe the system requirements, overall architecture, and innovative solutions found to the challenges presented by high-order AO on a segmented extremely large telescope. Further details may be found in specific papers on each of the observing modes and major subsystems.

Keywords: Extremely Large Telescopes, Adaptive Optics, Wavefront Sensing, Tomography, Laser Guidestar

1. INTRODUCTION

The Giant Magellan Telescope (GMT) is a 25.4 m diameter ground-based optical and infrared telescope being developed by a consortium of universities, research institutions, and national governments [1]. The telescope has a Gregorian optical design, with an $f/0.7$ primary mirror composed of seven 8.4 m diameter circular segments, an identically segmented concave secondary mirror (Fig. 1). The GMT will be built on Cerro Las Campanas, at Las Campanas Observatory in northern Chile. Preparation of the site has already begun, and construction is expected to begin in 2014.

Some of the GMT's highest science priorities require adaptive optics (AO) observing modes, which can provide vastly improved spatial resolution, sensitivity, and contrast over that allowed by natural seeing. However, as the potential gain provided by AO increases with aperture, so does the challenge. Alignment and vibration tolerances become tighter with

* abouchez@gmto.org; phone +1 626 204 0517; <http://www.gmto.org>

the smaller diffraction limit, and the required number of actuators, wavefront sensor subapertures, and guidestars increases.

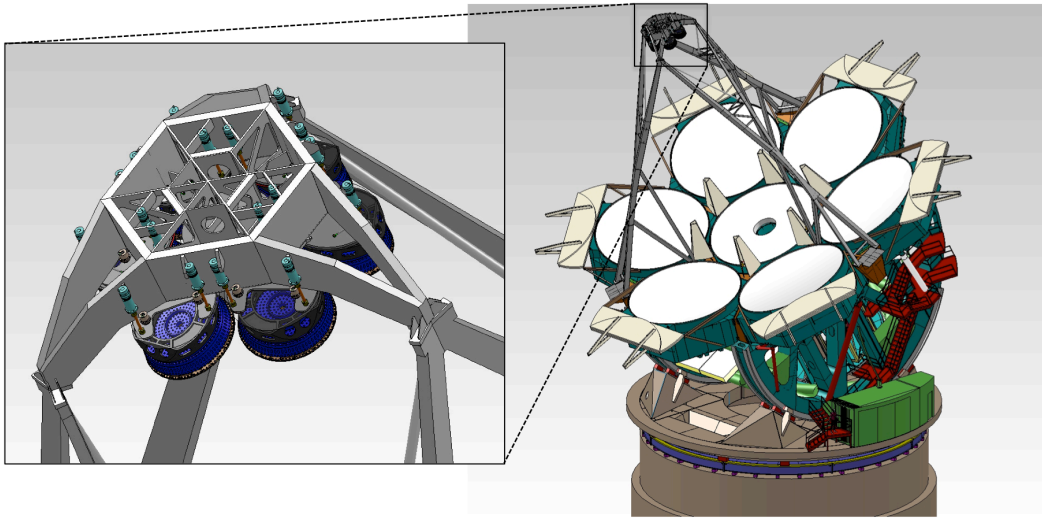


Fig. 1 : Rendering of the Giant Magellan Telescope (*right*) with a detail of the segmented Adaptive Secondary Mirror (*left*).

The GMT AO system is based on an Adaptive Secondary Mirror (ASM), which provides AO correction to *every* instrument on the telescope. Wavefront sensor assemblies at each telescope focus implement the AO observing modes required by the instruments at that location, similar to the MMT and LBT AO systems [2][3]. This design eliminates any common “AO relay” and provides high throughput and low emissivity, with a maximum of only 3 reflections between the sky and any instrument.

The GMT AO system is being developed as a collaboration between research groups at the GMT project office, the Australian National University, the University of Arizona, the Smithsonian Astrophysical Observatory, and Arcetri Observatory in Italy, together with industrial partners. This paper describes the requirements, system design, and development plans for the GMT AO system, and provides references to papers describing subsystems in greater detail.

2. AO MODES, REQUIREMENTS, AND ERROR BUDGETS

2.1 AO Observing Modes

The GMT AO system will provide 3 observing modes, which use different wavefront sensing approaches to balance turbulence compensation with sky coverage and field of view. The ASM provides wavefront correction for all modes:

- Natural Guide Star AO (NGSAO): The NGSAO observing mode uses a single pyramid natural guidestar (NGS) wavefront sensor to provide all of the wavefront correction information for the AO System, providing diffraction-limited imaging at 0.9-25 μm wavelength over a field of view limited by atmospheric anisoplanatism.
- Laser Tomography AO (LTAO): The LTAO observing mode uses a 1 arcmin diameter asterism of 6 Laser Guidestars (LGS) to tomographically reconstruct the high-order components of the atmospheric wavefront aberrations in the direction of a central science target. One faint natural guidestars must be used to measure tip-tilt, focus, segment piston, and dynamic calibration terms. The wavefront aberration will be compensated by the ASM, providing diffraction-limited imaging at 0.9-25 μm wavelength over a field of view limited by atmospheric anisoplanatism.
- Ground Layer AO (GLAO): The GLAO observing mode uses a wide guidestar asterism (either LGS/NGS or NGS-only) to detect and correct wavefront errors common to sky objects over a field of view up to 10 arcmin diameter. These errors are mainly due to low (up to 1 km) altitude components of the atmospheric wavefront aberrations. While providing some improvement in the visible, GLAO correction is expected to be particularly useful at wavelengths longer than 1 μm .

In addition to these AO observing modes, the ASM can be operated in a fast guiding mode (tip-tilt correction only) to support natural seeing observations, and a fixed mode for calibration.

Conceptual design studies for 6 GMT instruments were completed in October 2011 [4]. GMTNIRS, and GMTIFS, and TIGER are narrow-field diffraction-limited AO instruments designed to use the NGS AO and LTAO observing modes. NIRMOS, GMACS, and GCLEF are primarily natural-seeing instrument which can benefit from GLAO wavefront correction. In addition to these, a multi-instrument robotic fiber-feed system (MANIFEST) which would benefit from GLAO correction has also been proposed. The instruments are all mounted on a single large Gregorian Instrument Rotator (GIR), with narrow-field instruments fed by a tertiary mirror on its upper surface while wide-field instruments are located below and translated to the direct Gregorian focus (Fig. 2).

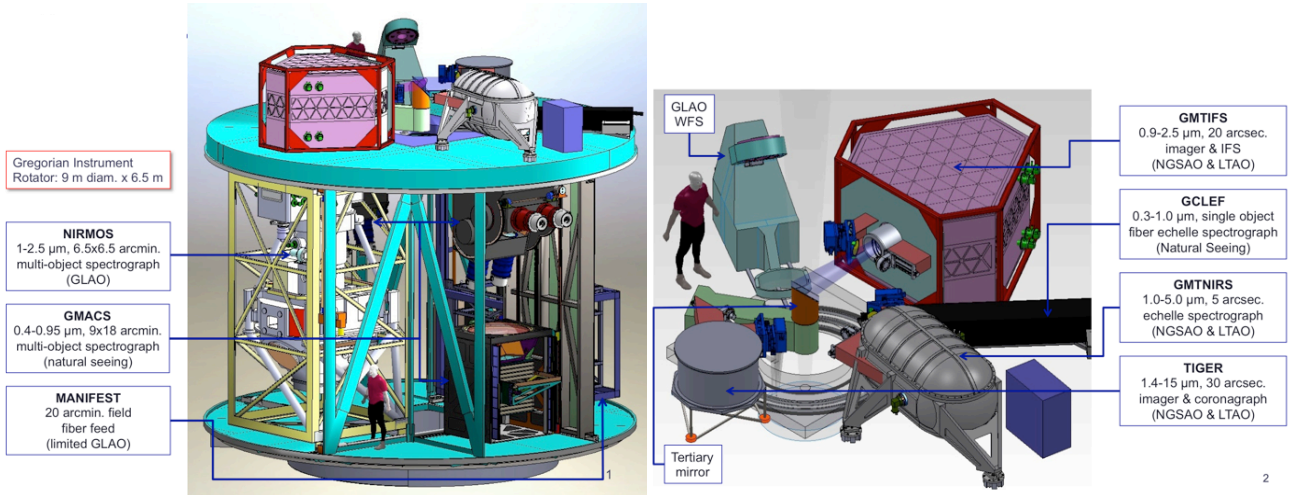


Fig. 2 : (Left) Proposed GMT wide-field instruments, mounted in the Gregorian Instrument Rotator (GIR). (Right) Proposed GMT narrow-field instruments and other subsystems mounted on the upper surface of the GIR.

2.2 Performance Requirements

The top-level performance requirements in each observing mode are listed in Table 1, and described in more detail in Trancho et al. [5]. The GMT AO performance requirements have deliberately been kept somewhat less ambitious than those of other extremely large telescope projects, allowing a comparatively simple and cost-effective design to meet those requirements. All performance requirements are specified at 15° from zenith median atmospheric conditions ($r_0=16.4$ cm at zenith), but with seasonal minimum sodium density (2.1×10^{13} atoms m^{-2}) and a conservative assumption of $L_0=60$ m turbulence outer scale.

Table 1: GMT AO Performance Requirements.

Mode	Performance Requirements
Natural Guide Star AO (NGSAO)	SCI-1883: >75% K Strehl for $R < 8$ stars. SCI-1882: $>10^5$ contrast at 0.12 arcsec ($4\lambda/D$) in L' band
Laser Tomography AO (LTAO)	SCI-1884: >30% H Strehl over 20% of sky at the galactic pole SCI-1885: >40% K ensquared energy in 50×50 mas over 50% of sky at the galactic pole SCI-1886: >50% K ensquared energy in 85×85 mas with $K=15$ on-axis NGS
Ground Layer AO (GLAO)	SCI-1887: <0.30 arcsec image FWHM at K band over >6.5 arcmin diameter SCI-4509: 15% image FWHM reduction in I band over >6.5 arcmin diameter

2.3 Error Budgets

Error budgets based on analytic calculations and confirmed using wave-optic simulations have been developed to flow down the top-level performance requirements to those of subsystems and components [5]. Examples for the NGS AO

and LTAO modes are shown in Table 2. The NGS AO mode must maintain <180 nm RMS high-order wavefront error, and <1.6 mas RMS tip-tilt error when using bright guidestars. We expect that this can be achieved with low risk by using a pyramid wavefront sensor with 92×92 subapertures across the pupil, and careful calibration [6].

The LTAO performance requirements are challenging, both in terms of high-order wavefront error and sky coverage. Requirement SCI-1884 implies a high-order error of <260 nm RMS, and tip-tilt error of <2.5 mas RMS. The high-order error includes the atmospheric component of segment piston, which is the difference in segment piston between the reconstructed wavefront and the true wavefront. Wavefront sensors based on geometric optics, such as the laser guide star Shack-Hartmann wavefront sensors, are unable to measure any piston error between the segments. Thus the atmospheric segment piston remains uncorrected, contributing ~110 nm RMS to the wavefront error budget [7]. Tomography error is the other dominant contributor, also approximately 110 nm RMS [8].

The LTAO mode’s 2.5 mas RMS tip-tilt error requirement at 20% sky coverage at the galactic pole is particularly challenging to meet in the presence of the ~15 mas RMS telescope wind shake expected in median (6.3 m/s) wind conditions [9]. The system design therefore relies on a diffraction-limited tip-tilt sensor operating in the K band, typically operating at 500 Hz frame rate. At 50% sky coverage at the galactic pole, the tip-tilt control requirement relaxes to ~10 mas RMS (SCI-1885).

Error budgets to the GLAO mode have been developed and are detailed in [5] and [10].

Table 2: Sample error budget for the NGS AO (left) and LTAO (right) observing modes.

Requirement Level	2	3	4	Requirements #			
High-Order Error							
AO High-Order aberrations	nm	125		AO-1763			
Atmospheric fitting	nm		70				
Temporal bandwidth	nm		70				
HO WFS measurement	nm		70				
Atmospheric Piston	nm		30				
Telescope Segment Piston	nm	30		AO-4424			
Static calibration	nm	64		AO-2861			
NGWFS optics	nm		30				
Instrument dichroic (reflection)	nm		32				
LGS dichroic (transmission)	nm		24				
Alignment (eg. WFS-to-ASM)	nm		20				
Field-dependent aberrations	nm		35				
Uncorrectable telescope aberrations	nm	30		TEL-2803			
Uncorrectable instrument aberrations	nm	50		INS-2802			
Contingency	nm		60				
Total high-order error	nm	155		SLR-1084			
Image motion							
AO Tip-tilt errors	mas	1.58		AO-1764			
Tip-tilt measurement	mas		1.00				
Tip-tilt temporal bandwidth	mas		0.50				
Atmospheric Dispersion	mas		0.50				
Residual flexure during exposure	mas		1.00				
Contingency	mas		0.50				
Total image motion	mas	1.58		SLR-1083			
Performance Metrics							
Strehl ratio	-	0.47	0.66	0.79	0.91	0.95	SCI-1883
FWHM	mas	10.0	13.5	17.8	28.9	38.7	

Requirement Level	2	3	4	5	Requirements #		
High-Order Error							
AO High-Order aberrations (Except Telescope Segment Piston)	nm		230		AO-1883		
Atmospheric fitting	nm			105			
Temporal bandwidth	nm			95			
HO WFS measurement	nm			75			
Tomography	nm			110			
Focus	nm			30			
Dynamic calibration	nm			45			
Atmospheric Piston	nm			110			
Telescope Segment Piston	nm	50			AO-4422		
AO Static calibration	nm	64			AO-2862		
LWFS optics	nm			30			
Instrument dichroic	nm			32			
LGS dichroic (VWFS Frame)	nm			24			
Alignment (eg. WFS-to-ASM)	nm			20			
Field-dependent aberrations	nm			35			
Uncorrectable telescope aberrations	nm	30			TEL-2803		
Uncorrectable instrument aberrations	nm	50			INST-2802		
Contingency	nm		70				
Total high-order error	nm	251			SLR-1088		
Image motion							
AO Tip-tilt errors	mas		2.1		AO-1762		
Tip-tilt measurement	mas			1.5			
Tip-tilt temporal bandwidth	mas			0.5			
Tip-tilt anisokinetism	mas			1.3			
OIWFS tip-tilt errors	mas			0.3			
Residual centroid anisoplanatism	mas				0.2		
Residual atmospheric dispersion	mas				0.1		
Residual flexure during exposure	mas				0.2		
Contingency	mas		2.2				
Total image motion	mas	2.1			SLR-2804		
Performance Metrics							
Strehl ratio	-	0.16	0.36	0.56	0.80	0.88	SCI-1884
FWHM	mas	10.1	13.6	17.8	28.9	38.7	

3. AO SYSTEM ARCHITECTURE

The GMT AO system design is based on a common adaptive secondary mirror (ASM), and wavefront sensors assemblies replicated for each instrument. All narrow-field AO instruments are located at the Folded Gregorian ports provided by a steerable tertiary mirror which passes a 180 arcsec diameter field. Each instrument cryostat window is a long-pass dichroic, and all visible-light wavefront sensing is performed in the beam reflected by the window (see Fig. 3). This light is further divided between a patrolling NGS AO wavefront sensor and an LTAO wavefront sensor by a fixed notch dichroic. In the NGS AO mode, all wavefront aberrations are sensed by a single NGS AO WFS are corrected by the

ASM. In the LTAO observing mode, the tomographically reconstructed high-order wavefront from the LTAO WFS is combined with tip-tilt, focus, segment piston, and dynamic calibration errors sensed by an NGS On-Instrument Wavefront Sensor. These drive the ASM, uplink tip-tilt control to the LGS Facility, and an open-loop micro-electro-mechanical (MEMS) deformable mirror built into the On-Instrument Wavefront Sensor. In all AO modes, the facility Acquisition, Guiding, and Wavefront Sensors (AGWS) at the direct Gregorian focus use measurements of 3 NGS outside of the central AO field of regard to control gravitational and thermal distortion of the primary mirror segments.

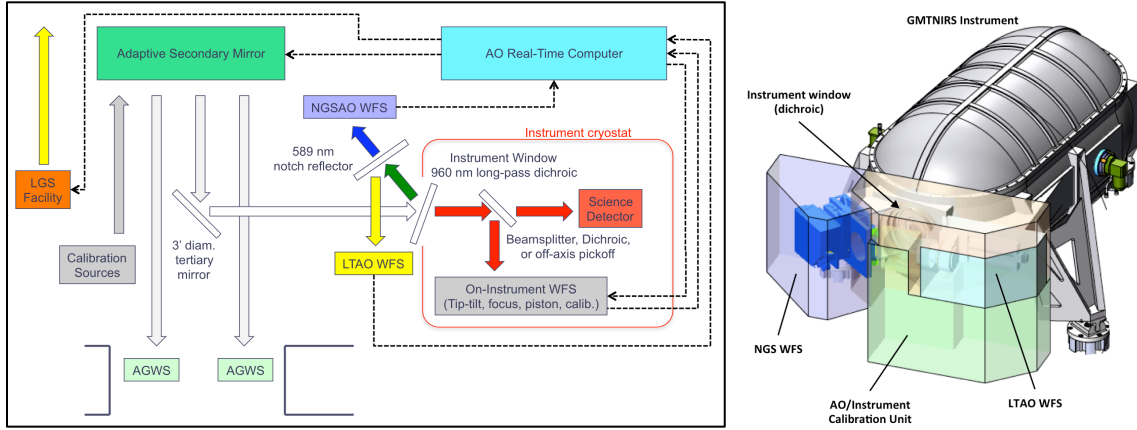


Fig. 3 : (Left) Block diagram of the NGS AO and LTAO modes. Light paths are shown with wide arrows, control signals with dashed arrows. (Right) Schematic arrangement of the NGS AO and LTAO wavefront sensors attached to the front of a science instrument.

There are two GLAO observing modes, used only by wide-field instruments which can be translated to the direct Gregorian focus (Fig. 4). The NGS GLAO (NGLAO) mode uses 3 NGS, sensed by the AGWS in the periphery of the direct Gregorian field, to control both the ASM at moderate bandwidth and the primary mirror support actuators at slow rates. This mode inserts no optics in the beam and is compatible with any direct Gregorian instrument, including those which use the facility wide-field corrector/ADC. The LGS GLAO mode (LGLAO) provides higher performance over a narrower field of view. It is implemented by inserting a large tilted notch dichroic in the beam ahead of the instrument, and sensing the LGS with a set of 6 WFS. The AGWS are used to measure tip-tilt, focus, and dynamic calibration errors.

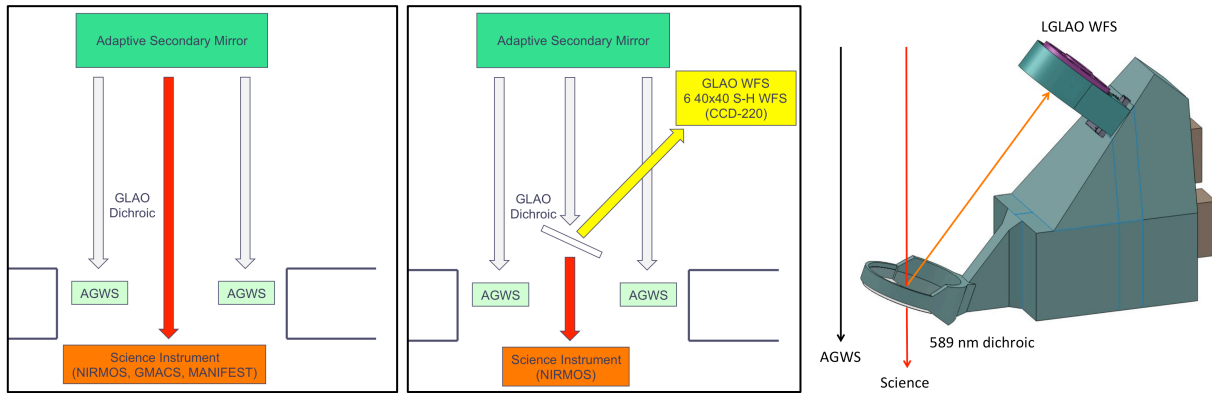


Fig. 4 : (Left) Block diagram of the NGS GLAO (NGLAO) observing mode. (Center) Block diagram of the LGS GLAO (LGLAO) observing mode. (Right) Rendering of the LGLAO wavefront sensor assembly.

4. AO SUBSYSTEMS

4.1 Adaptive Secondary Mirror

The Adaptive Secondary Mirror (ASM) forms the common correcting element of all AO observing modes of the GMT. It is being developed by a consortium of Microgate Srl. and ADS International. The ASM is composed of six identical 1.04 m diameter off-axis and segments, and one 1.05 m diameter on-axis segment. Each has 672 voice coil actuators

(4704 total), actuating a 2 mm thick Zerodur face sheet at up to 1 kHz update rate. Capacitive sensors maintain the shape of the face sheet with respect to a lightweighted Zerodur reference body with ~ 3 nm precision. The actuators are coupled magnetically to the face sheet, leading to the very desirable property that poorly-controlled or failed actuators exert no force and can be removed from the control with little reduction in performance.

The GMT ASM design is based closely on that of the VLT [11], but with improved reference body support, less onboard computation, and higher-efficiency voice coil motors. We also intend to implement an advanced actuator control scheme with a dynamic feed-forward term to further improve the mirror's dynamical behavior [12].

4.2 Laser Guidestar Facility

High-order wavefront sensing in the LTAO and LGLAO observing modes will be provided by 6 sodium laser guidestars. We performed an extensive trade study comparing the expected performance of on-axis and off-axis LGS launch architectures [8]. We concluded that the additional readout noise due to the greater elongation in the off-axis case was compensated by the fact that each wavefront sensor observes the LGS elongated in a different direction at a given location in the pupil. Slowly-varying calibration errors due to changes in the structure of the sodium layer, which are amplified by greater elongation, can be mitigated by measuring centroids with a larger number of pixels in each wavefront sensor subaperture. In the absence of a significant performance penalty, we selected the off-axis launch architecture because it eliminates LGS fratricide and allows a major simplification in the design of the beam transfer and launch systems. Thus our baseline design uses therefore six 20 Watt Raman fiber lasers to be coupled directly to six 38 cm diameter refractive launch telescopes, located in 3 pairs at the ends of the stiff primary mirror cell connector frame (Fig. 5). The laser and launch telescope designs follow closely the Very Large Telescope AO Facility design.

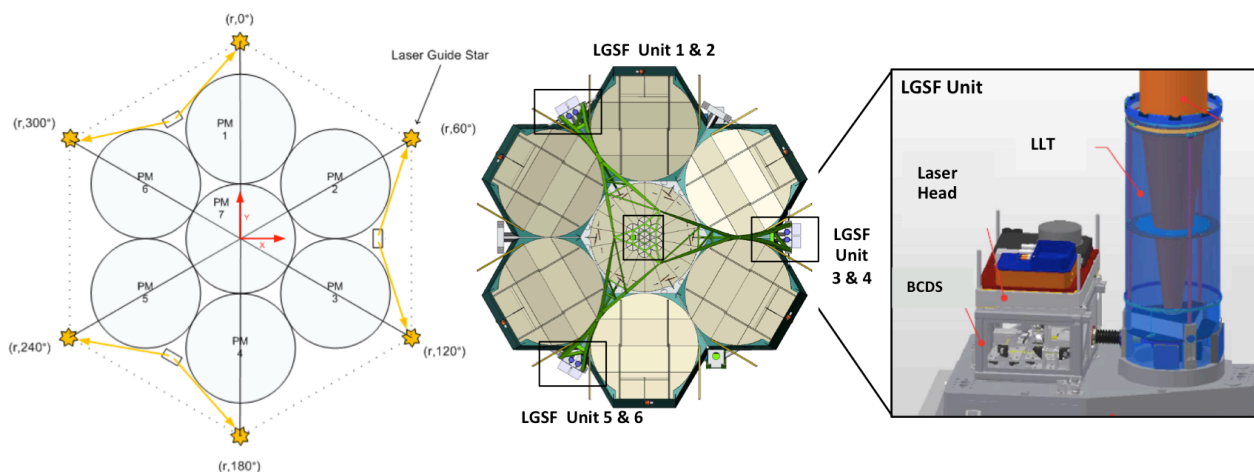


Fig. 5 : (Left) Schematic of the 3 launch locations and 6 laser guidestars in LTAO mode, projected onto the pupil. (Center) Rendering of the GMT primary mirror with mirror covers closed and Laser Guidestar Facility Units indicated. (Right) Rendering of a single LGSF Unit (image courtesy of TNO).

Analyses of the expected photon return and spot size have been performed, based on the detailed photon return simulations published by Holzlöhner et al. [13]. At 15° zenith angle, we expect a return flux of 407 ± 51 photons $\text{cm}^{-2} \text{s}^{-1}$ at the telescope primary in seasonal minimum sodium conditions (2.1×10^{13} atoms m^{-2}), and ~ 1.0 arcsec FWHM spot size.

4.3 Natural Guidestar Wavefront Sensor

Wavefront sensing in the NGS AO mode will be provided by a pyramid natural guidestar wavefront sensor (NGWS) housed in the Visible Wavefront Sensor Assembly attached to the front of each narrow-field AO instrument (Fig. 3). The NGWS design and predicted performance are described in detail in Esposito et al. [6]. The 92×92 pupil sampling of the detector matches the average actuator density of the ASM (0.29 m), leading to an atmospheric fitting error of 61 nm RMS in median conditions if all available modes are controlled. The NGWS includes an atmospheric dispersion corrector, modulation of the image on the pyramid using a tip-tilt mirror, a K-mirror rotator, and pupil steering optic to stabilize the pupil on the E2V CCD-220 detector (Fig. 6, left). The sensor has a 180 arcsecond diameter un-vignetted patrol field.

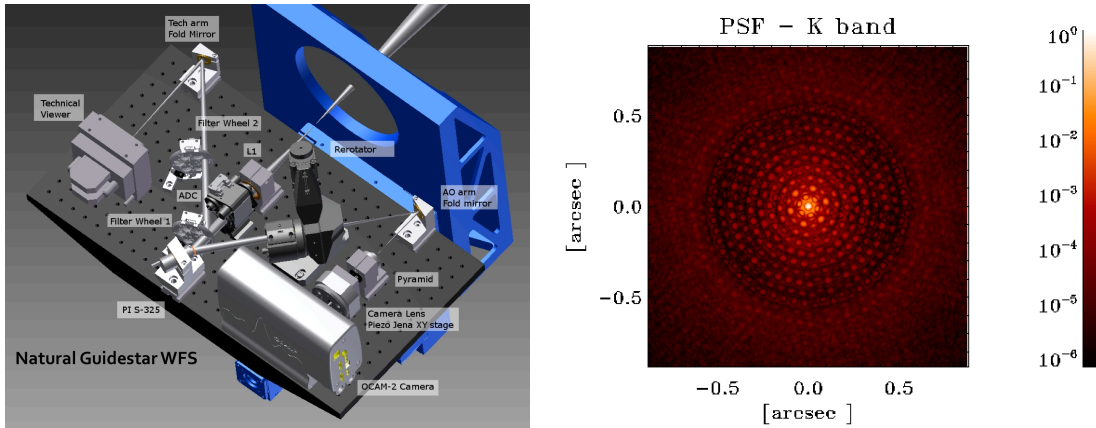


Fig. 6 : (Left) Opto-mechanical design of the Natural Guidestar WFS. The gray breadboard patrols a 180 arcsec diameter field on 3 linear stages. (Right) Simulated PSF for a bright guidestar in median conditions, when controlling only 2500 modes. The K band Strehl is 90.5%.

The choice of a pyramid WFS was based on two factors: the high sensitivity and low aliasing demonstrated by current systems, and the predicted ability of the pyramid to phase the GMT segments. Segment piston caused by incorrect positioning of the primary or secondary mirror segments, and that due to random atmospheric phase delays, must both be sensed by the NGWS and corrected at high bandwidth by the ASM. The ability of the pyramid to achieve this in the GMT case has been supported by detailed simulations, though in poor seeing it may be necessary to use an external large capture range piston sensor (see Section 5) to resolve phase wrapping ambiguities. Further simulations and a laboratory prototype are planned. With phase wrapping does not occur, the predicted performance of the NGWS far exceeds specifications for bright guidestars, delivering wavefront error as low as 110 nm RMS in median conditions in the absence of wind shake or vibration (Fig. 6, right).

4.4 Laser Tomography Wavefront Sensor

The laser tomography wavefront sensor (LTWS) will provide tomographic high-order wavefront sensing in the LTAO observing mode. The selected design and alternatives considered are described in [8] and [14]. The LTWS consists of 6 60×60 Shack-Hartmann wavefront sensors co-mounted in a rotation bearing and on a long-travel focus stage to track the LGS asterism, which remains fixed with respect to the telescope pupil and varies in range from 82.5 to 200 km (Fig. 7). The asterism diameter is fixed at 30 arcsec radius, providing a balance between the on-axis and off-axis tomographic reconstructions (see Section 4.5). Each camera uses a 840×840 pixel NGSD CMOS detector currently under development by E2V to provide 14×14 pixels and a field of view of 9.2 arcsecond in each subaperture.

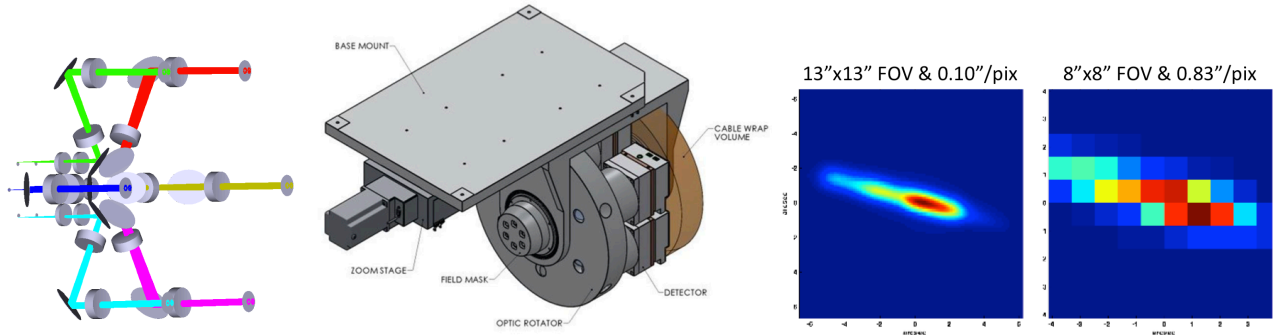


Fig. 7 : (Left) Optical design of the Laser Tomography WFS, illustrating the 6 channels. (Center) Mechanical design of the assembly, which rotates to track the rotating LGS asterism. (Right) Example noiseless images of the most elongated LGS spot, with a typical sodium density profile. The $0.83''/\text{pix}$ image is similar to that which the GMT LTWS will record ($0.71''/\text{pix}$ and 9×9 arcsec FOV).

Extensive simulations have been performed to optimize the LTWS design [8] [15]. The system has been specified to meet the error budget requirement of 260 nm RMS high-order wavefront error in seasonal minimum sodium conditions, which requires operation at 500 Hz framerate with an estimated ~ 600 detected photocounts/subaperture at 15° zenith

angle. In higher photon return conditions, the system can be operated at up to 1 kHz framerate. The design maintains aberrations due to changes in the sodium layer density structure to <30 nm RMS by adequately sampling the elongated LGS.

4.5 On-Instrument Wavefront Sensor

An infrared on-instrument wavefront sensor (OIWFS) housed within each LTAO science instrument is the sole natural guidestar sensor required for the LTAO mode [8] [16]. The design of the OIWFS is not as advanced as other subsystems, but its requirements are well established. It must sense 4 types of aberrations at different rates, using guidestars as faint as $K=18$:

- Tip-tilt at 100-500 Hz
- Focus at 10 Hz
- Segment piston at >0.1 Hz
- “Truth” sensing (20-30 modes) at >0.03 Hz

The OIWFS must also be modular to accommodate instruments requiring only on-axis LTAO reference stars (TIGER and GMTNIRS) and those using off-axis guidestars to provide high sky coverage (GMTIFS). The off-axis version will include a 1024-actuator MEMS deformable mirror to compensate the anisoplanatism experience by off-axis guidestars. This MEMS DM is controlled in open-loop, using an independent tomographic reconstruction. This reduces the wavefront error seen by the OIWFS when 60 arcseconds off-axis from 800 to ~350 nm RMS [8].

One possible candidate for this MEMS-corrected OIWFS is a tip-tilt guider operating in the K band, and an unmodulated 10×10 infrared pyramid wavefront sensor operating in the H band, split by a dichroic [16]. The tip-tilt channel would use a Teledyne HAWAII2-RG detector with 35 mas/pixel plate scale and multi-accumulate quad-cell readout. The pyramid WFS would also use a HAWAII2-RG (potentially the same detector) to measure focus, segment piston, and higher-order wavefront errors all at 10 Hz. Detailed performance simulations with randomly-generated starfields indicate that this design can meet the LTAO performance requirements, providing 20% sky coverage at the galactic pole for diffraction-limited imaging, and will far exceed the sky coverage requirements for AO spectroscopy with large spaxels (see Fig. 8).

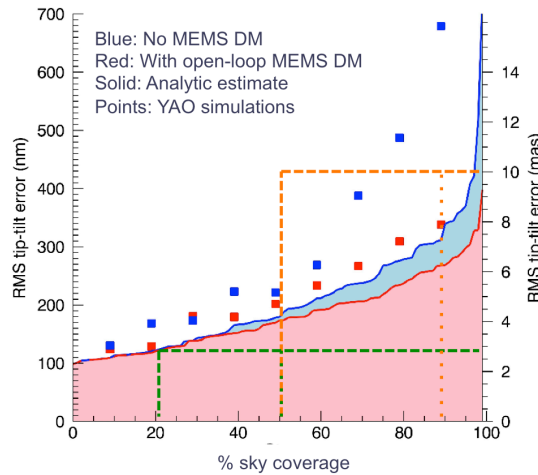


Fig. 8 : Predicted tip-tilt performance of the LTAO On-Instrument Wavefront Sensor. The 2.5 mas RMS tip-tilt error requirement for diffraction-limited H band imaging (SCI-1884) requires a MEMS DM run in open loop to achieve 20% sky coverage at high galactic latitude (green lines). Such a system also delivers >90% sky coverage for spectroscopy with 50 mas spaxels (orange lines at 10 mas RMS, consistent with requirement SCI-1885).

4.6 Natural Guidestar GLAO Wavefront Sensors

The NGLAO mode will be implemented using the facility Acquisition, Guiding and Wavefront Sensors which patrol the direct Gregorian focal plane ahead of the wide-field instruments. The mode requires only 3 Shack-Hartmann wavefront sensors with 1-2 m subapertures sampled at ~100 Hz to correct the lowest altitude turbulence using a tomographic reconstructor which optimizes the image quality over a wide (5-10 arcmin diameter) field of view [10]. The AGWS

sensors, using electron-multiplication CCDs, would have a limiting magnitude of $R=17.5$ and thus nearly 100% sky coverage using guidestars located near the periphery of the science field. Predicted performance is quite attractive given the simplicity of the potential implementation: From an uncorrected FWHM of $0.364''$ in K (assuming median conditions and $L_0=60$ m), to $0.220''$ across a 6.5 arcmin diameter field (if using 2 m subapertures). No opto-mechanical design of the AGWS has yet been performed, but their requirements do appear to be overly challenging.

4.7 Laser GLAO Wavefront Sensors

A set of Laser GLAO wavefront sensors will provide higher performance GLAO correction over somewhat narrower fields of view, at the expense of increase complexity and some reduction in throughput. The Laser GLAO WFS assembly can be deployed ahead of infrared instruments located at the direct Gregorian focus (Fig. 4, right), providing improved seeing-limited images over a 4 to 6.5 arcminute diameter FOV. A 60 cm diameter long-pass dichroic reflects the LGS to an assembly consisting of 6 40×40 Shack-Hartmann wavefront sensors co-mounted in a rotation bearing and on a long-travel focus stage, and transmits wavelengths greater than 600 nm to the science instrument. Sensing of tip-tilt, focus, and dynamic calibration errors is performed with the AGWS, which patrol the annulus outside of the dichroic. While the specifications of the wavefront sensors are significantly relaxed due to the smaller number of subaperture and more relaxed error budget compared to LTAO, the large dichroic is challenging to manufacture and to support.

The performance of an LGLAO system is likely to exceed that of NGLAO over field view smaller than ~ 6.5 arcmin diameter, and be more resilient to uncertainties in the turbulence distribution since tomographic reconstruction is unnecessary (Fig. 9).

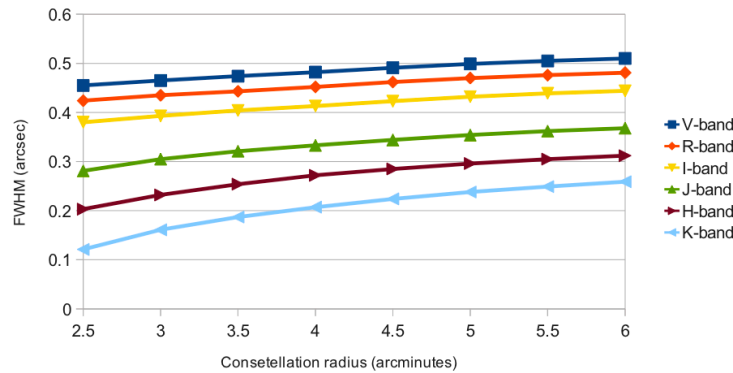


Fig. 9 : Predicted LGLAO performance vs. LGS asterism radius in median atmospheric conditions. While the image quality improvement is greatest in the near-infrared, some improvement is apparent in the visible. The uncorrected FWHM is 0.57/0.54/0.51/0.45/0.40/0.36 arcsec in V/R/I/J/H/K bands.

5. SEGMENT PHASING

Achieving the diffraction limit of the 25.4 m GMT will require the primary and secondary mirrors to be phased to <50 nm RMS. Due to the large separation between primary segments (30-40 cm) and their construction of borosilicate, capacitive or inductive edge sensors alone are not expected to be sufficiently stable over timescales longer than a few minutes. In the NGS AO observing mode, the NGWS can sense and correct segment piston at up to 1 kHz. However, only faint natural guidestars are generally available in the LTAO mode. We have therefore designed a 3-stage phasing system consisting of a coarse optical phasing sensor with a large capture range to initially phase the telescope and detect phase wrapping of the OIWFS, primary and secondary mirror metrology systems to maintain alignment over short timescales, and a high-sensitivity optical sensor in the OIWFS to correct long-term drifts in the edge sensors [17]. No phasing is required in the GLAO or Natural Seeing observing modes.

The coarse phasing sensor will be a dispersed Hartmann design, with 1.6 m subapertures spanning the 12 inter-segment gaps. It will patrol the direct Gregorian focus ahead of the wide-field instruments (and outboard of the tertiary mirror, if deployed), similar to the AGWS. The light from the two segments passing through each aperture interferes, forming fringes on a Hawaii-2RG detector in the K band. A grism disperses the fringes at low spectral resolution ($R \sim 60$), increasing the sensor's capture range to $>20 \mu\text{m}$. A prototype of the coarse phasing sensor has been built at the Smithsonian Astrophysical Observatory, and will be tested on the Magellan Clay telescope later this year [18]. It has

demonstrated 50 nm RMS segment piston sensitivity in the lab, using an artificial sources equivalent to the guidestars expected to be available ($R=15$).

The design for the primary mirror edge sensors uses 48 commercial distance measuring interferometers to sense the relative motions of mirror segments on short timescales (Fig. 10) [19]. These are located in crossed pairs at 24 locations between the primary mirror segments, mounted to bosses machined in the mirror side walls with retro-reflecting corner cubes mounted on the opposite segment. We expect this arrangement to achieve ~ 2 nm RMS sensitivity to piston excursions caused by vibration and wind buffeting.

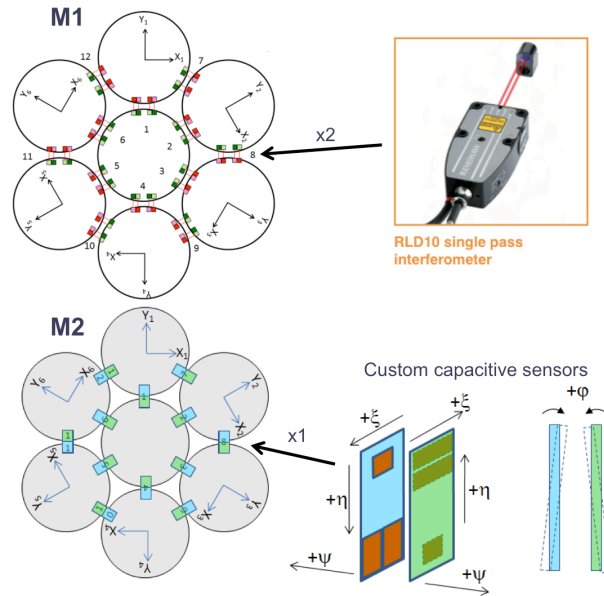


Fig. 10 : (Top) Primary mirror edge sensor concept, using 48 off-the-shelf distance-measuring interferometers. (Bottom) Secondary mirror edge sensor concept, using 12 custom capacitive sensors capable of each measuring 5 degrees of freedom.

More compact capacitive sensors will be used to sense relative displacements between the adaptive secondary mirror reference bodies. Twelve of these sensors will be mounted in the gaps between the ASM reference bodies, each sensing 4 degrees of freedom using an arrangement of custom split-plate capacitors working across a 5 mm gap. These sensors will maintain the segments to ~ 6 nm RMS in piston, and ~ 10 nrad in relative tilt, over timescales of hours.

In the LTAO observing mode, the primary and secondary mirror metrology systems will detect rapid changes in segment tilt and piston, which must be compensated in a feed-forward mode using the agile ASM face sheet actuators. Slow drifts in the edge sensors will be detected by the OIWFS, and corrected by modifying the setpoint of the metrology sensors. For a more detailed discussion of the phasing control loops and error budget, see [17].

6. AO CONTROLS DESIGN

With a large number of wavefront sensors and a deformable mirror integrated into the telescope, the GMT AO system can greatly benefit from a distributed controls architecture. Each wavefront sensor will have associated with it a slope computer which converts pixel values into local wavefront slope measurements. The slope vectors will be transferred to a central real-time computer (RTC) using a commercial low-latency switching network such as Mellanox Infiniband. Communications between the RTC and ASM will follow the same protocol.

The LTAO observing mode is the most demanding in terms of throughput and computational power, while high-contrast observations in the NGS AO mode demand the lowest latency. We intend to use a Linear Minimum Mean Square Error (LMMSE) reconstructor [8], which will require 3 Gb/s maximum data throughput on the network and 75 Gflop of computing power. Rapid advances in highly parallel computing architectures have recently made several attractive RTC options available, including single-board GPU and CPU solutions. We intend to prototype both options later in 2012, with the goal of selecting a baseline design prior to preliminary design review.

7. INTEGRATION

A test tower is being designed to facilitate optical testing of the ASM segments, and integration of the full AO system, prior to shipment to the observatory (Fig. 11). A retro-reflector can be inserted at prime focus, and illuminated by an interferometer at the Gregorian focus. Alternately, fiber sources can be inserted at prime focus (including 6 sources mimicking the LGS asterism) and used to close the control loops on the wavefront sensors. Interfaces replicating those of the telescope will be provided, allowing all AO and instrument functionality to be tested during the integration phase. Once integration is complete, the test tower will be shipped to the observatory and installed in a purpose-built room in the base of the telescope enclosure. If extended maintenance or recalibration of the ASM is necessary, the ASM frame can be lowered directly from the telescope onto the tower.

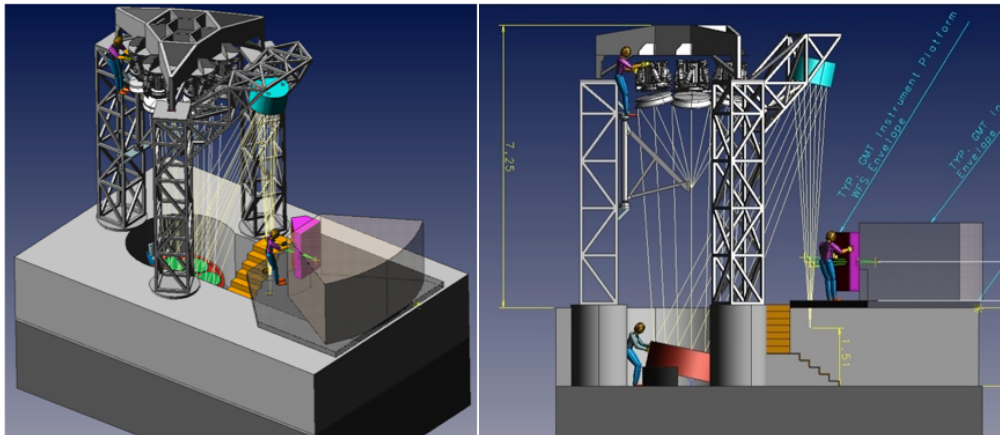


Fig. 11 : Conceptual design of the ASM test tower, which will also be used to integrate and test the full system including narrow-field AO instruments.

8. CONCLUSIONS

The GMT AO system is currently in the preliminary design phase, leading to a System Preliminary Design in early 2013. Construction approval in early 2014 would allow the installation of the lasers on the telescope in 2019 and the ASM in mid-2020. This would be followed by approximately 1 year of commissioning of the AO observing modes.

While uncertainty remains in the design of some subsystems (particularly the OIWFS and RTC), we feel confident that we have identified an overall design which will meet the GMT AO performance requirements while maintaining relative simplicity and future upgradability. We plan to prototype several of the high-risk components, including the OIWFS DM, ASM actuators, and phasing metrology systems over the next year. We will also begin developing concepts for second generation GMT AO capabilities, coordinated with the second generation of GMT instrumentation which may be solicited as early as 2016.

ACKNOWLEDGMENTS

This work has been supported by the GMTO Corporation, a non-profit organization operated on behalf of an international consortium of universities and institutions: Astronomy Australia Ltd, the Australian National University, the Carnegie Institution for Science, Harvard University, the Korea Astronomy and Space Science Institute, the Smithsonian Institution, The University of Texas at Austin, Texas A&M University, University of Arizona and University of Chicago. This material is based in part upon work supported by AURA through the National Science Foundation under Scientific Program Order No. 10 as issued for support of the Giant Segmented Mirror Telescope for the United States Astronomical Community, in accordance with Proposal No. AST-0443999 submitted by AURA.

REFERENCES

- [1] Johns M., McCarthy, P. J., Raybould, K., Bouchez, A., Farahani, A., Filgueira, J. M., Jacoby, G., Shtetman, S., Sheehan, M., "Giant Magellan Telescope: Overview," Proc. SPIE 8444, (2012).
- [2] Hart, M., Milton, N. M., Baranec, C., Powell, K., Stalcup, T., McCarthy, D., Kulesa, C., Bendek, E., "A ground-layer adaptive optics system with multiple laser guide star," Nature 466, 727-729 (2010).
- [3] Esposito, S., Riccardi, A., Fini, L., Puglisi, A. T., Pinna, E., Xompero, M., Briguglio, R. Quirós-Pacheco, F., Stefanini, P., Guerra, J. C., Busoni, L., Tozzi, A., Pieralli, F., Agapito, G., Brusa-Zappellini, G., Demers, R., Brynnel, J., Arcidiacono, C., Salinari, P., "First light AO (FLAO) system for LBT: final integration, acceptance test in Europe, and preliminary on-sky commissioning results", Proc. SPIE 7736, (2010).
- [4] Jacoby, G. H., Bouchez, A. H., Colless, M., DePoy, D. L., Fabricant, D. G., Hinz, P. M., Jaffe, D. T., Johns, M., McCarthy, P. J., McGregor, P. I., Shtetman, S. A., Szentgyorgyi, A. H., "The instrument development and selection process for the Giant Magellan Telescope," Proc. SPIE 8446, (2012).
- [5] Trancho, G., Espeland, B., Bouchez, A. H., Conan, R., Hinz, P. M., van Dam, M. A., "GMT AO system requirements and error budgets in the preliminary design phase," Proc. SPIE 8447, (2012).
- [6] Simone Esposito, S., Pinna, E., Quirós-Pacheco, F., Puglisi, A. T., Carbonaro, L., Bonaglia, M., Biliotti, V., Briguglio, R., Agapito, G., Arcidiacono, C., Busoni, L., Xompero, M., Riccardi, A., Fini, L., Bouchez, A., "Wavefront sensor design for the GMT natural guide star AO system," Proc. SPIE 8447, (2012).
- [7] van Dam, M. A., Hinz, P. M., Codona, J. L., Hart, M., Garcia-Rissmann, A., Johns, M. W., Shtetman, S. A., Bouchez, A. H., McLeod, B. A., Rigaut, F., "Modeling the adaptive optics system for the Giant Magellan Telescope," Proc. SPIE 7736-42, (2010).
- [8] Conan, R., van Dam, M. A., Espeland, B., Uhlendorf, K., Piatrou, P. K., Bennet, F. H., Bouchez, A., "The Giant Magellan Telescope laser tomography adaptive optics system," Proc. SPIE 8447, (2012).
- [9] Sheehan, M., Gunnels, S., Johns, M. W., Hull, C. L., Kern, J., Shtetman, S. A., "Progress on the preliminary structural and mechanical design of the Giant Magellan Telescope," Proc. SPIE 8444, (2012).
- [10] Hinz, P. M., Brusa-Zappellini, G., Vaitheeswaran, V., McMahon, T., Connors, T., Knox, R. P., Montoya, M., Bouchez, A. H., "Design and predicted performance of the GMT ground-layer adaptive optics mode," Proc. SPIE 8447, (2012).
- [11] Biasi, R., Andrighttoni, M., Angerer, G., Mair, C., Pescoller, D., Lazzarini, P., Anaclerio, E., Mantegazza, M., Gallieni, D., Vernet, E., Arsenault, R., Madec, P.-Y., Duhoux, P., Riccardi, A., Xompero, M., Briguglio, R., Manetti, M., Morandini, M., "VLT deformable secondary mirror: integration and electromechanical tests results," Proc. SPIE 8447, (2012).
- [12] Manetti, M., Morandini, M., Mantegazza, P., "GMT Adaptive Secondary Mirror Servo-Fluid-Elastic Simulation", GMT internal report (2010).
- [13] Holzlöhner, R., Rochester, R. H., Pfrommer, T., Banaccini Calia, D., Budker, D., Highbie, J. M., Hackenberg, W., "Laser guide star return flux simulations based on observed sodium density profiles," Proc. SPIE 7736 (2010).
- [14] Wang, M., Kristina Uhlendorf, K., Jones, D. J., Côté, P., Châteauneuf, F., Gauvin, J., Conan, R., Espeland, B., "Optical designs with LGS WFS system for GMT-LTAO," Proc. SPIE 8447, (2012).
- [15] van Dam, M. A., Conan, R., Bouchez, A. H., Espeland, B., "Aberrations induced by side-projected laser guide stars in laser tomography adaptive optics systems," Proc. Adaptive Optics for Extremely Large Telescopes (2011).
- [16] van Dam, M. A., Conan, R., Bouchez, A. H., Espeland, B., "Design of a truth sensor for the GMT laser tomography adaptive optics system," Proc. SPIE 8447, (2012).
- [17] Bouchez, A. H., McLeod, B. A., Acton, D. S., Kanneganti, S., Kibblewhite, E. J., Shtetman, S. A., van Dam, M. A., "The Giant Magellan Telescope phasing system," Proc. SPIE 8447, (2012).
- [18] Kanneganti, S., McLeod, B. A., Ordway, M. P., Shtetman, S. A., Bouchez, A. H., Codona, J., Eng, R., Gauron, T. M., Norton, T. J., Roll, Jr., J. B., Streechon, P., Weaver, D., "A prototype phasing camera for the Giant Magellan Telescope," Proc. SPIE 8447, (2012).
- [19] Acton, D. S., Bouchez, A. H., "Phasing metrology system for the Giant Magellan Telescope," Proc. SPIE 8444 (2012).